Implementation of a Low-Latency Contention-Free Geographical Routing Scheme for Mobile Cyber-Physical Systems

Implementation of a Low-Latency Contention-Free Geographical Routing Scheme for Mobile Cyber-Physical Systems

***Abstract*—Results and lessons learned from the implementation of a novel ultra low-latency geo-routing scheme are presented in this paper. The geo-routing scheme is intended for team-based mobile cyber-physical systems whereby a cluster of unmanned vehicles (robots) are deployed to accomplish a critical mission under human supervision. The contention-free nature of the developed scheme lends itself to jointly achieve lower latency and higher throughput. Implementation challenges are presented and corresponding resolutions are discussed herewith.**

***Index Terms*—team-based mobile cyber-physical systems, unmanned aerial vehicles (UAV), mobile ad hoc networks (MANET), contention-free geo-routing, blind cooperative transmission, carrier frequency offset (CFO), software-defined radios (SDR).**

I. Introduction

A special class of cyber-physical systems entails the deployment of teams of autonomous robots (unmanned vehicles) as well as human agents to accomplish certain critical missions [1]. Within such a context, swarms of unmanned aerial or terrestrial vehicles are dispatched into the field to conduct a mission under human supervision or control, or in other instances jointly with human agents.

A broad spectrum of applications are possible. Examples include the use of a swarm of unmanned aerial vehicles (UAV) for thermal imaging and remote sensing [2]. UAV clusters have been also considered for 3D mapping, surveying, and other civil engineering tasks [3]. Swarms of terrestrial robotic agents are also being increasingly considered for some time-critical field operations most notably for search and rescue and tactical missions [4]. Another manifestation of team-based mobile cyber-physical systems includes task-oriented teams of paramedics and first responders during disasters or massively crowded events. The availability of real-time video communications for those scenarios is indeed a powerful tool for collaborative decision-making and optimal mission execution [5].

A paramount task for team-based mobile cyber-physical system is the joint planning and optimization of motion trajectories of the mobile nodes [6]. The timeliness of disseminating path planning and control signalling messages is crucial [4]. Hence, end-to-end latency is a major performance metric [7]. UAV-based cyber-physical systems are typically not bandwidth-hungry. The converse is true however for terrestrial systems whereby real-time video communication is sought between the team members. As a special case of mobile ad-hoc networks (MANET), team-based mobile cyber-physical systems undoubtedly push the envelope in terms of latency and throughput requirements.

Indeed, MANET is a well-established research field that is at least a couple of decades old. MANET research space further evolved to cover vehicular and flying ad hoc networks (VANET and FANET respectively). Multihop packet routing has always been at the forefront of MANET, VANET, and FANET research challenges. Geographical routing (geo-routing) has been widely adopted in the context of MANET due to its resilience to mobility and network topological changes [8]. As a matter of fact, geo-routing has been embraced by the European Telecommunications Standards Institute (ETSI) as a standard VANET routing technique for Intelligent Transport Systems (ITS) [9]. However, this paper advocates the need to revisit the status-quo of geo-routing techniques. This is mainly driven by the ultra low latency constraints and high capacity requirements associated with mobile cyber-physical applications. Current implementations of geo-routing are unfortunately plagued by an overhead that grows rapidly with node density and/or frame arrival rate [10]. This indeed has adverse consequences on latency and throughput performance. Such an issue has already been identified and prioritized as a serious challenge in the context of mobile ad hoc networks [11], [12].

One direction which is quite promising, yet still poorly exploited is the hybrid use of "blind cooperative relaying" in conjunction with geo-routing. Blind cooperative relaying was formally introduced for the first time by [13]. The relaying mechanism was actually dubbed there as "randomized distributed cooperative transmission". In essence, blind cooperative relaying entails the forwarding of physical frames while not reverting to any relay selection process. The term *blind* mainly stems from the fact that nodes within a cooperative cluster are actually unaware of each other [14]. In other words, there is not any sort of cross-coordination between nodes before the frame is transmitted.

As will be shown in the next section, blind cooperative relay actually paves the way for an entirely contention-free geo-routing scheme. As a bonus, it also offers two types of link gains: array (power) and diversity gains. Array gain is due to multiple nodes jointly transmitting the same packet. Diversity gain on the other hand can be achieved via use of randomized transmit precoding matrices [13]. It is however beyond the scope of this implementation and is deferred as a future work item.

The main contribution of this paper is to demonstrate the implementation feasibility of contention-free geo-routing for mobile cyber-physical systems. The paper is organized as follows. The need to design a contention-free geo-routing scheme for mobile cyber-physical systems is further motivated in Section II. Implementation challenges and means to resolve

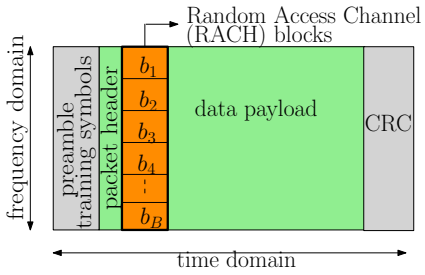

Fig. 1. A random access channel is inserted into the OFDM frame to allow concurrent transmitters to stamp their position information.

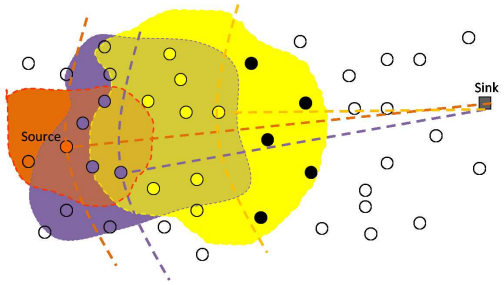

Fig. 2. Illustration of the operation of the contention-free geo-routing scheme. A source injects a frame into the network. Receivers who are closer to the sink than the source relay the frame. In the second hop, each receiver goes through position information conveyed by the transmitters of the first hop to decide whether to forward the frame or not. Any second-hop receiver which offers positive progress towards the sink will decide to forward.

them are presented in Section III. Test results obtained from the field and lessons learned are reported in Section IV. Conclusions and future work are outlined in Section V.

II. Contention-Free Geo-Routing

A. Overview

Broadly speaking, classical geo-routing may take one of two forms [15]:

1) Beacon-based whereby position beacons are exchanged among neighboring nodes, so as to maintain up-to-date topological awareness.
2) Beaconless such that receiver-based contention takes place to select the packet forwarder.

Both cases however suffer from the aforementioned large overhead problem. This is either due to message exchange overhead for beacon-based protocols [16], or due to contention resolution overhead in the beaconless case [17].

The underlying routing overhead can be eliminated by devising a contention-free beaconless geo-routing mechanism. The basic building block is the use of blind cooperative relaying whereby multiple nodes concurrently[1] transmit the same frame. To handle the artificial multipath created by such concurrent transmission, the transceivers must employ an orthogonal frequency division multiplexing (OFDM) physical layer. As long as signal copies from concurrent transmissions arrive within the guard interval of the OFDM symbol then the signal can be decoded properly.

On the other hand, each node has to be equipped with the localized capability of qualifying whether it makes positive progress towards the sink or not. This was addressed in detail in [10]. At a given hop i, nodes concurrently transmitting a frame need to convey their position information to the receivers. This is accomplished by means of a random access channel (RACH) which is inserted into the frame structure as illustrated in Figure 1. Each node randomly selects one of the B available blocks to encode its position information. A receiver must scan through these blocks to extract the position information of the transmitters. Accordingly, each node locally decides whether to forward the frame or not. The contention-free geo-routing scheme is further illustrated and described in Figure 2.

[1]This is true at the packet-level time scale. At the symbol-level however, the cooperative transmitters are not perfectly aligned in time thereby causing inter-symbol interference (ISI) at the receiver.

Obviously collisions may occur. If there are I concurrent transmitters, the probability that no collisions occur (i.e. each RACH block contains a unique position attribute) is given by:

$$p_u = \left(\frac{B-I}{B-I+1}\right)^{\frac{I(I-1)}{2}}. \quad (1)$$

RACH blocks with collisions are discarded by the receiver. The receiver extracts the position information contained in other blocks and compares them to its own position. The geo-routing rule applied by a receiver herewith is to forward if it is simply closer to the sink than all transmitting nodes.

When a collision occurs on one or more RACH blocks, the likely effect is that nodes *not* offering positive progress will forward the packet. As a consequence, this leads to the following two paradoxical effects:

1) Having more nodes engaged in the transmission is equivalent to a larger array gain and consequently a larger communication range. This in return results in reducing the end-to-end latency (Section II-B).
2) It results in increasing the aggregate energy consumed per hop to forward a frame. However, it does not necessarily result in a higher end-to-end energy consumption per frame since the boost in communication range results in reducing the total number of hops.

The energy-latency tradeoff driven by collision events was investigated rigorously in [10]. It was specifically shown that contention-free geo-routing is poised to consume more end-to-end energy at very high node density and large geographical spans. Both conditions are generally not applicable in the case of mobile cyber-physical systems. Anyway, to put things into the right context, the probability of extra energy consumption due to collisions is not a major concern here. Unmanned vehicles are equipped with high-capacity batteries to support their mechanical moving parts. On the other hand, missions involving humans tend to be relatively short in duration such that battery recharge frequencies are sufficient to disregard this dilemma.

B. Performance Gains

The performance of contention-free geo-routing in terms of three key metrics is now contrasted to classical contention-based schemes. The goal is to a establish without any doubt the fact that contention-free geo-routing is far more optimal for MANET applications.

The metrics considered are end-to-end latency, maximum achievable throughput, and broadcast reachability. Latency and throughput are obviously crucial metrics affecting the quality of service for real-time communications. Broadcast teachability is important for upstream quality control and configuration messages that are sent out from the sink. In this paper, the superiority of contention-free geo-routing in terms network throughput is established for the firs time.

1) End-to-End Latency: The end-to-end latency is $\sum_{i=1}^{q} T_i$ where q denotes the expected number of hops and T_i is the duration of the ith hop. The array and diversity gains made available by blind cooperative transmission (in the case of contention-free geo-routing) eventually result in reducing the total number of hops, q. In the case of contention-free geo-routing the hop duration is deterministic. It is equal to the packet duration T_p plus a turn-around time T_{TAT} corresponding to the change from receiver state to transmitter state. On the other hand, in the case of contention-based geo-routing the sender needs to select the farmost receiver. The selection is established through a handshake process that consists at the bare minimum of [15]:

1) Request-to-send message of duration T_{RTS} followed by a turnaround time T_{TAT}.
2) A clear-to-send message from the optimal receiver with duration $T_{CTS} = T_{RTS}$ followed by T_{TAT}.
3) Packet transmission with duration T_p.

The hop duration is therefore $T_i \geq T_p + 2T_{TAT} + 2T_{RTS}$ which is always greater than that of the contention-free case. Hence, it is straightforward to conclude that contention-free geo-routing offers significantly lower end-to-end latency [10].

2) Maximum Achievable Throughput: An absorption probability p is defined as the probability that a node is the destination of a packet given that the node has received the packet from its neighbors [18]. The expected number of hops traversed by a packet between its source and destination is simply $q = 1/p$ [18]. The mobile cyber-physical network can be modeled as a random access multihop network assuming the use of carrier sense multiple access with collision avoidance (CSMA/CA). In [19], it was shown that the maximum achievable throughput per node, R_{max}, is given by:

$$R_{max} = \frac{L_p}{q\left[cT_b + T_p(1+4NA)\right]}, \tag{2}$$

where[2]

$$c = \begin{cases} q & \text{contention} - \text{based} \\ 1 & \text{contention} - \text{free} \end{cases}.$$

In (2), L_p is the packet length in bits, T_b is the average back-off time, N denotes the number of nodes in the network, and A is the average coverage area for a packet transmission. An increase in the communication range by a factor of a yields reduction in q by an approximately a factor of a but an increase in the coverage footprint area by a factor of a^2. Therefore, in light of (2), contention-free geo-routing may offer a throughput gain under the condition of appreciable drops in the average back-off time T_b.

In order to analyze T_b, the key question to be addressed: during the entire multihop journey of a given packet, what is the average number of nodes, $\overline{M}$, who are forced to queue at least one packet transmission? This is important since the back-off probability $P_b = \overline{M}/N$ and hence the mean back-off time is $T_b = \left(\frac{N}{N-\overline{M}}\right) T_w$, where T_w is the waiting time before reattempting to transmit.

To tackle this problem, the probability that exactly m nodes will back off during a given hop is analyzed. Given n nodes exist in the back-off region and a packet arrival rate of l_A, then this probability is given by:

$$p_m(m|n) = \binom{n}{m} \left(1 - e^{-T_i l_A}\right)^m \left(e^{-T_i l_A}\right)^{n-m}, m \leq n. \tag{3}$$

The probability that exactly n nodes actually exist in the region is $p_n(n) = \frac{1}{n!}(\rho A)^n e^{-\rho A}$, where ρ is the network node density. Consequently, the probability distribution function of m is given by $p_m(m) = \sum_{n=m}^{\infty} p_m(m|n) p_n(n)$. The next question to tackle: in light of the above, what is the probability, $P_M(M)$, that M sensor nodes backlog at least one transmission during the q-hop lifetime of the packet in concern? The different permutations for distributing those M nodes over q hops can be conveniently computed using integer set partitioning algorithms. These permutations can be expressed in matrix format as

$$\begin{bmatrix} m(1,1) & \dots & m(1,q) \\ \vdots & \ddots & \vdots \\ m(\mathcal{P},1) & \dots & m(\mathcal{P},q) \end{bmatrix} \in \mathbb{Z}^{\mathcal{P}\times q}, \tag{4}$$

where $\mathcal{P}$ equals the number of different permutations corresponding to the distribution of M back-off nodes over q hops. Consequently, the probability density function is obtained as follows:

$$P_M(M) = \sum_{u=1}^{\mathcal{P}} \prod_{i=1}^{q} p_m(m(u,i)). \tag{5}$$

Therefore, a compact expression for $\overline{M}$ can be obtained as follows:

$$\overline{M} = \sum_{M=0}^{\infty} \sum_{u=1}^{\mathcal{P}} \prod_{i=1}^{q} \sum_{n=m(u,i)}^{\infty} M p_m(m|n) p_n(n). \tag{6}$$

Using (2) - (6), the ratio of R_{max} for contention-free geo-routing to that of contention-based was computed. A terrestrial application was assumed such that the large-scale path loss coefficient, α, can be taken in the range of $[2.7 - 3.5]$ [20]. The coefficient α was adjusted such that each transmission was carried out on average by three nodes. Results are shown in Figure 3.

Although a larger a is indeed in favor of lower end-to-

[2]It is noteworthy to mention that the factor c is missing from Eq. (22) in [19]. While CSMA/CA is applied only once at the source in case of contention-free routing, it is applied at each intermediate hop in case of contention-based geo-routing.

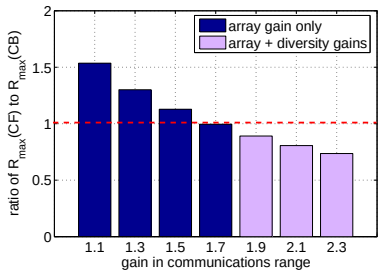

Fig. 3. The maximum achievable throughput per node for the case of contention-free divided by that of contention-based geo-routing. The computation was carried out assuming a network of 40 nodes at a density of $\rho = \frac{1}{82}\text{m}^{-2}$. The communication range was ≤ 25m at a path loss coefficient of 2.8. Packet duration of 1ms at an arrival rate of 30s^{-1}.

Fig. 4. An SDR platform from Nuand was used to build the contention-free geo-routing protocol.

end latency, it is not always preferable in terms of throughput performance. It is evident from the figure that contention-free geo-routing starts to lose its edge in terms of per-node capacity as the the gain in communication range, a, increases. Nonetheless, empirical results obtained from field testing and reported in Section IV reveal that the maximum link gain obtainable solely from the array gain of three transmitters is 6 dB. Accordingly, the maximum reach gain was measured to be $a = 1.77$. From Figure 3, contention-free geo-routing yields higher throughput per node for the range $a \leq 1.7$. However, when proper randomized transmit coding is applied, then a diversity gain of at least 3 dB is expected [13], thereby further boosting a but causing the throughput ratio to increasingly decline.

Based on the above, a straightforward conclusion that can be drawn: randomized diversity coding should be used only to boost latency performance of contention-free geo-routing at the expense of losing its edge in terms of maximum achievable throughput.

3) Broadcast Reachability: The last performance metric considered here is broadcast reachability. Contention-based geo-routing offers better broadcast reachability for three intuitive reasons:

1) Larger communication range due to the array and diversity gains [21].
2) Shorter hop duration and lower end-to-end latency [21].
3) Higher number of nodes engaged on average in a given packet transmission.

Furthermore, the time duration required to reach a desired level of reachability can be also straightforwardly shown to be a decreasing monotone in all of the aforementioned parameters.

III. Implementation Challenges

A. Hardware and Software Platform

The clear-cut advantages of contention-based geo-routing were sufficiently motivating to explore its feasibility in terms of hardware and software implementation. Since the scheme invokes significant changes into the PHY frame structure, off-the-shelf OFDM modems could not be used. Instead, a software-defined radio (SDR) platform is utilized. The BladeRF SDR platform (www.nuand.com) was selected. The BladeRF houses a 40KLE Altera Cyclone IV field programmable gate array (FPGA) as well as a Cypress microcontroller on board. The analog front-end (AFE) is a full-fledged reconfigurable chip from Lime Microsystems. A radio frequency (RF) amplifier from Texas instruments was annexed to the BladeRF as shown in Figure 4 such that the maximum RF transmit power is 9 dBm. The physical layer (PHY) algorithms were developed in VHDL on the FPGA while the medium access and geo-routing decisions were embedded on the microcontroller. The system was built using a 128-point OFDM PHY. The sampling frequency used is 10 MHz. The guard interval consists of 32 samples such that the total number of samples per symbol is 160. The center frequency was chosen to be 2450 MHz.

B. Challenges and Resolutions

Two major issues that have proved to be most challenging during the implementation are discussed herewith.

1) RACH Implementation: The signal of a non-empty RACH block is composed of the superposition of the position information of one or more relays. Each RACH block is randomly picked by a unique set of relays. As such, each RACH signal undergoes a different channel towards a given receiver. Therefore, RACH signals are generally expected to be non-aligned in time, as illustrated in Figure 5.

Time misalignments of the RACH symbols occur due to the variations in propagations delays between the relays towards the receiver in concern. A RACH OFDM symbols is the aggregation of all the RACH incoming signals. As shown in Figure 5, the receiver aligns its time reference to the first energy arrival of the first OFDM symbol. The first OFDM symbol in the packet is the preamble symbol. The receiver locks to the first energy arrival of the preamble symbol, which happens to be that of the 2nd relay in this example. Hence, for some RACH blocks the FFT processing window at the receiver will not be aligned in time to the actual start of the RACH signal of that block.

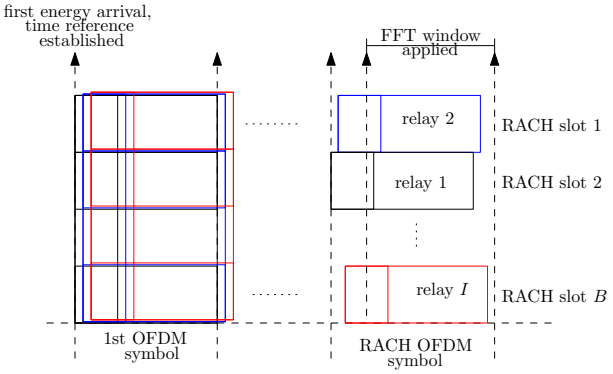

Fig. 5. Illustration of the time offset problem on the RACH portion of the frame.

Fortunately, this is not a source of concern since it only results in a mere phase rotation. The effect of time offset on the detection of OFDM symbols was studied in detail in [22]. It was shown that when the time offset is "towards" the guard interval, i.e. the FFT window is partially applied on the guard interval. Accordingly, only a phase error is introduced. Interestingly, it is only time offsets *towards* the guard interval that are possible in the case of contention-free geo-routing.

Using differential modulation eliminates the effect of the time offset problem. Reverting to differential modulation for RACH processing fortunately comes at an affordable price:

1) It is computationally affordable. The increase in code space on the FPGA is marginal. The other option was to reuse the readily available coherent modulation module. However, this requires to prefix each RACH block with its own preamble sequence to estimate individual channels along with the associated distortions due to time offsets. Evidently, this comes at the expense of significant computational footprint on the FPGA and therefore was disregarded.
2) The use of differential modulation is associated with a signal to noise ratio (SNR) penalty. Nevertheless, there is a $10 \log B$ dB power boost on RACH blocks. This is true since the whole RF power is focused on the RACH block of choice at each transmitter. This indeed compensates for the SNR penalty.

2) Carrier Frequency Offset (CFO) Spread: The composite channel model corresponding to joint frame transmission by I nodes is depicted in Figure 6. The sampling frequency is $1/T_s$, and n is a running sample index. The transmitted signal goes over I indecently channels, corresponding to the concurrent transmitters. Each individual channel consists of a multipath tap-delay line with L taps such that the total delay spread is $(L-1)T$. The delays ${T_1}', \ldots, {T_I}'$ correspond to the propagation delays towards the receiver. The number of subcarriers is denoted by N_s. Moreover, the CFO between transmitter i and the receiver is denoted by δ_i such that $x_i \triangleq e^{j2\pi\delta_i T_s}$. The transmitted baseband signal is expressed as:

$$s(nT_s) = \sum_{k=-\frac{N}{2}}^{\frac{N_s}{2}} a_{k,n} e^{j\phi_{k,n}} e^{j2\pi k \Delta f n T_s}. \quad (7)$$

Consequently, the bandpass received signal is given by:

$$r(nT_s) = \sum_{i=1}^{I} \sum_{l=1}^{L} {x_i}^n s(nT_s) \cdot h_{i,l} e^{j2\pi f_c (nT_s - {T_i}') - (l-1)T)} + {\sigma_w}^2, \quad (8)$$

where ${\sigma_w}^2$ is the noise power. Although the fading coefficients are assumed to be quasi-static, but the CFO spread makes the frequency-domain response of the composite channel time-varying:

$$H_n(f) = \sum_{i=1}^{I} {x_i}^n e^{-j2\pi f {T_i}'} \sum_{l=1}^{L} h_{i,l} e^{-j2\pi f (l-1)T}. \quad (9)$$

In cases of mobility, δ_i also includes an additional component corresponding to the doppler shift. The CFO spread is expressed as $\max_i \delta_i - \min_i \delta_i$. In UAV-based systems, clocks may be conveniently disciplined by GPS signals. However, for terrestrial applications the GPS signal is often unavailable. As such, the CFO problem exists and in fact may have detrimental effects. As a matter of fact, the CFO spread effect is far more adverse than the doppler spread since it can be orders of magnitude larger.

This is better appreciated by means of an example. The CFO shift with free-running clocks was measured to be in one instance in the range of ± 2000 Hz (1ppm). In comparison, the maximum doppler shift is given by v/λ, where v is the velocity of the node and λ is the wavelength. With maximum velocities in the range of 30 - 40 km/hr for UAV-based applications, the doppler shift is less than 90 Hz. Consequently, it is evident that the CFO spread problem is far more challenging than the classical doppler spread. The channel coherence time (roughly equal to the reciprocal of the maximum doppler shift) in case of free-running clocks is actually in the range of only a few OFDM symbols. Channel estimation and equalization at the receiver has therefore to cater for such a highly dynamic and fast-changing conditions.

One approach to update the channel coefficients estimate is by means of inserting training symbols more frequently within the frame. However, the coherence time is significantly smaller than the frame duration. As such this will cause the PHY overhead due to pilots to grow significantly. A neater approach is to blindly estimate the channel in a continuous fashion using the well-known decision-directed estimation (DDE) method [23]. Here, the $(j-1)$th equalized symbol is used to construct an estimate of the channel response at the jth symbol. Assuming zero-forcing equalization, the channel estimate is given by $\widehat{H}_j(f) = R_j(f)/\widehat{S}_j(f)$, where $S_j(f)$ and $R_j(f)$ are the fourier transforms of the transmitted and received jth symbol respectively. The equalized jth symbol is obtained by $\widehat{S}_j(f) = R_j(f)/\widehat{H}_{j-1}(f)$.

In addition to the use of the DDE method, the system implementation also utilizes a pilot structure similar to that

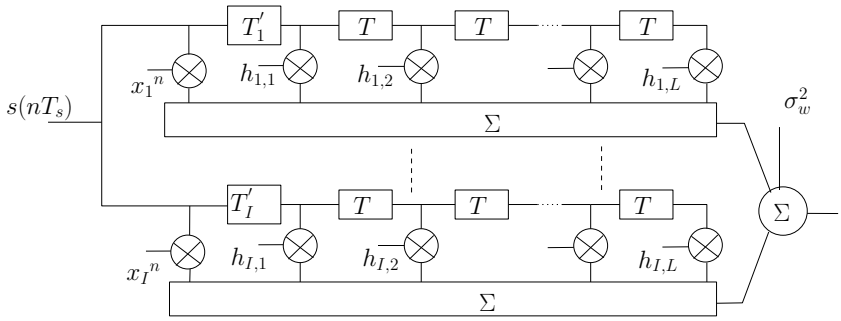

Fig. 6. Composite channel response capturing CFO / doppler spread, propagation delay differences, as well as multi-path reflections.

implemented in the IEEE 802.11a standard. A total of 8 pilot tones are used for residual phase tracking. Pilot-based tracking and DDE work together in a complementary fashion.

IV. Field Test Results

Generally, the core challenge in conjunction with any mobile system is to handle the time-varying channel characteristics. It was shown in Section III that the CFO spread produces a channel that is much more dynamic than that produced by doppler spread, even at high speeds. A corollary to this is the fact that empirical results collected from the field under CFO spread with *stationary* nodes are sufficient to ensure the implementation will successfully handle mobility.

It is also worthwhile to emphasize that topological changes in a MANET are due to fluctuations in individual link SNR values and not because of translational movements of nodes. This is better appreciated by a simple numerical example. If the coherence time of the channel is 500μs, then assuming 1ms packets (which is the case in this implementation) the SNR may drop significantly during a single packet transmission, thus causing a link loss. However, the relative change in positions between two neighboring nodes is quite insignificant during a 1ms interval. For two nodes which are 50-meters apart and traveling at 10m/s (36km/hr), the maximum change in their separation is only 0.2%.

To validate the quality of implementation, the following tests were carried out.

A. RACH Processing

A threshold detector is employed on each RACH block at the output of the FFT module. If the threshold is exceeded, then the differential demodulation processing module is activated. The test scenario was to have 8 nodes transmit concurrently. In this specific test case, each block was comprised of 8 subcarriers spanning 5 consecutive time symbols. The first symbol is a phase reference symbol for the differential modulation.

Each node was configured to select one of 5 adjacent RACH blocks. Adjacency is important to test the performance of the detection and demodulation modules under the high likelihood of inter-carrier interference (ICI). The 8 nodes were placed equidistantly from the sink. Furthermore, 4 nodes were configured to select the same RACH block while each of the remaining 4 was to uniquely select one of the remaining blocks.

Results of this test are shown in Figure 7(a).It is noted that the successful detection rate of the unique RACH blocks was greater than 99%. Such a successful detection rate is particularly satisfactory for the 4th RACH block since it suffers from relatively high ICI from the adjacent collision block. It was also quite intriguing to see that the the number of noise instances on the collision block was so high (exactly 1252), although the average aggregate received power on this specific block is 6 dB higher. A root cause analysis revealed that the higher received power feeds the FFT module with an input that is beyond the $\pm$1v acceptable range. Consequently, the FFT module yields a highly distorted output, which may mislead the threshold detection module to consider it as noise.

It is also noted that collisions were recorded on the unused RACH blocks. This corresponds to the situation where the detection threshold is exceeded but no useful position information is contained.

B. DDE Performance

The performance of the DDE implementation was investigated under a controlled setup. A dedicated BladeRF board was configured to feed 3 other boards with two common signals: clock and trigger, as shown in Figure 8. The latter is used to instruct the 3 relays to commence the transmission of a frame that is pre-stored on the FPGA. The CFO is invoked locally at each transmitting node via the command line interface. Similarly, each node my be configured to introduce a fixed delay after the rising edge of the trigger signal. This can be used to produce the desired delay spread for the composite channel. In other words, it helps control the propagation delays $T_1{}', \ldots, T_I{}'$.

In this test, the three transmitters were placed 12 meters from the receiver. The CFO spread was varied and the frame error rate (FER) at the receiver was logged with and without DDE. As expected, DDE is quite a viable tool to equalize time-varying channels [23]. A sample result is provided in Figure 9 whereby the received baseband I/Q stream at the receiver is plotted for both cases. In this specific test instance the CFO values ranged between -100 Hz and 1000 Hz. The

(a) A screenshot displaying the cumulative detection results on the RACH blocks.

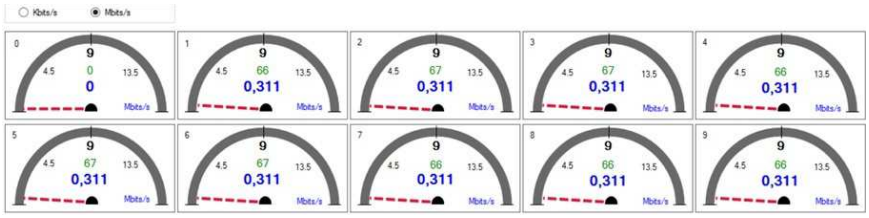

(b) A screenshot of the GUI's speedmeter. Real-time streaming from 9 nodes towards the sink, showing a sustained throughput of 310 kbps for all streaming nodes.

Fig. 7. Snapshots taken from the graphical user interface developed to diagnose, control, and configure the nodes.

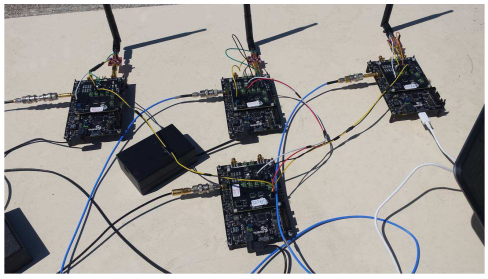

Fig. 8. Common clock and trigger signals are fed into the boards. The controlled test setup is used to measure the performance of the decision-directed equalization method.

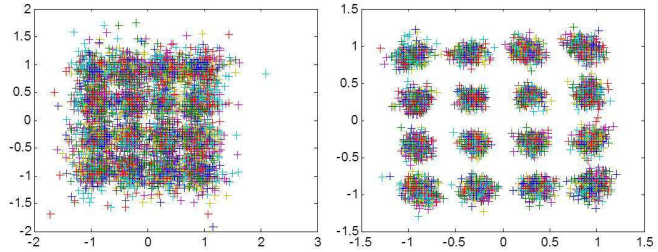

Fig. 9. DDE performance investigated for the case of concurrent transmission from three nodes with CFO_1 = 1000 Hz, CFO_2 = 0 Hz, CFO_3 = -100Hz. Here, the received I/Q symbols is plotted.

FER plunged from 81% down to less than 5% thanks to using the DDE module at the receiver.

C. Array Gain

The goal of this test case was to measure the array gain as well as the maximum reach gain that can obtained by means of blind cooperative transmission. To obtain the maximum reach gain, the CFO is forced to zero on all three transmitters. The three transmitters were always kept equidistant from the receiver.

TABLE I
RESULTS FROM THE ARRAY GAIN TEST.

	SNR (dB)	RSSI (dBm)	FER	reach (meters)
Tx_1 only	16.4	-88.2	2.9%	65
	12.4	-93.1	50.8%	115
Tx_2 only	16.5	-87.5	0.8 %	65
	11.2	-94.1	76.2 %	115
Tx_3 only	16.1	-88.0	1.1%	65
	11.8	-93.5	47.0%	115
all	18.3	-86.7	2.0%	115

The first stage of this stage was to measure the communication range for each individual transmitter at a FER target of 3%. The range obtained was 65 meters as shown in Table I. Next, the communication range for the case of three concurrent transmitters was measured by moving the receiver away. The maximum range was measured to be 115 meters, i.e. the reach gain was 50 meters or equivalently 77%.

In order to characterize the array gain, each transmitter was placed 115 meters away from the receiver and the SNR was measured. The array gain is simply the difference between the SNR obtained under joint transmission and the average of individual SNR values. It is clear from Table I that blind cooperative transmission is able to offer nearly 6 dB of array gain.

D. Real-time Streaming

The final test entailed real-time packet streaming from 9 nodes in a multihop fashion towards the sink. The nodes were

positioned arbitrarily within a 50x10 meters rectangular strip. the RF transmit power was scaled down to 0 dBm. The set of neighbors of node n is denoted by $\mathcal{N}(n)$ and defined as the set of nodes within the communication range of an individual transmission. The subset containing neighbor offering positive progress towards the sink is denoted by $\mathcal{N}^+(n) \subset \mathcal{N}(n)$. At a transmit power level of 0 dBm, it was verified that $|\mathcal{N}^+(n)| = 1$. In other words, there was no node which had more than one neighbor closer than itself towards the sink. Nodes in this test were configured to use 16 QAM$\frac{3}{4}$ and a data payload of 1950 KB. The total frame duration was ≈1ms at an arrival rate, l_A = 20 s^{-1}. Medium access method used at the source was CSMA/CA.

A sustained throughput of 311 kbps was attained for each of the 9 nodes as shown in Figure 7(b). Depending on the position of the source relative to the sink, the number of hops traversed by frames ranged from 1 to 5. With a turn-around time T_{TAT} of less than 180μs, the contention-free geo-routing implementation provided an end-to-end latency of 5.72 ms at most. With such an ultra-low latency figure, particularly relative to the packet arrival rate, the CSMA/CA module rarely went into a back-off state on any node. This therefore explains the uniformity of the achieved streaming rate across all 9 nodes. Such a sustained bit rate was shown in a separate test to be quite sufficient to stream H.264 video at 15 frames per second and a frame resolution of 640x480.

V. Conclusions

Team-based mobile cyber-physical systems are envisioned for a multitude of industrial, civilian, and law-enforcement applications, often involving real-time video streaming. As such, end-to-end latency and maximum achievable throughput per node have paramount important in these systems. Of all network design components, multihop routing is by far the key design metric.

Contention-based geo-routing has been often advocated in the context of mobile ad hoc networks. Nonetheless, contention-free geo-routing has been analytically proven in this paper to push the performance envelope even further. As such, there was a strong motivation to take contention-free geo-routing from theory to practice. The paper presents a rather detailed insight into the challenges and lessons learned from the implementation of contention-free geo-routing on a software-defined radio platform. Numerous field test cases were carried out to validate its feasibility and established its added value.

References

[1] J. Fink, A. Ribeiro, and V. Kumar, "Robust control for mobility and wireless communication in cyber-physical systems with application to robot teams," *Proceedings of the IEEE*, vol. 100, no. 1, pp. 164–178, Jan 2012.

[2] J. Berni, P.J. Zarco-Tejada, L. Suarez, and E. Fereres, "Thermal and narrowband multispectral remote sensing for vegetation monitoring from an unmanned aerial vehicle," *Geoscience and Remote Sensing, IEEE Transactions on*, vol. 47, no. 3, pp. 722–738, March 2009.

[3] Sebastian Siebert and Jochen Teizer, "Mobile 3d mapping for surveying earthwork projects using an unmanned aerial vehicle (uav) system.," *Automation in Construction, Elsevier*, vol. 41, Feb 2014.

[4] J. Fink, A. Ribeiro, and V. Kumar, "Robust control of mobility and communications in autonomous robot teams," *Access, IEEE*, vol. 1, pp. 290–309, 2013.

[5] A. Panayides, Z.C. Antoniou, Y. Mylonas, M.S. Pattichis, A. Pitsillides, and C.S. Pattichis, "High-resolution, low-delay, and error-resilient medical ultrasound video communication using h.264/avc over mobile wimax networks," *Biomedical and Health Informatics, IEEE Journal of*, vol. 17, no. 3, pp. 619–628, May 2013.

[6] I. Bayezit and B. Fidan, "Distributed cohesive motion control of flight vehicle formations," *Industrial Electronics, IEEE Transactions on*, vol. 60, no. 12, pp. 5763–5772, Dec 2013.

[7] Ilker Bekmezci, Ozgur Koray Sahingoz, and SAmil Temel, "Flying ad-hoc networks (fanets): A survey.," *Ad Hoc Networks, Elsevier*, 2013.

[8] Xiaojing Xiang, Xin Wang, and Zehua Zhou, "Self-adaptive on-demand geographic routing for mobile ad hoc networks," *Mobile Computing, IEEE Transactions on*, vol. 11, no. 9, pp. 1572–1586, Sept 2012.

[9] "Intelligent transport systems (its); vehicular communications; geonetworking; part 4: Geographical addressing and forwarding for point-to-point and point-to-multipoint communications; sub-part 1: Media-independent functionality, v1.2.0," Oct 2013.

[10] A. Bader, K. Abed-Meraim, and M.-S. Alouini, "An Efficient Multi-Carrier Position-Based Packet Forwarding Protocol for Wireless Sensor Networks," *IEEE Transactions on Wireless Communications*, vol. 11, no. 1, pp. 305 – 315, Jan 2012.

[11] A.A. Abouzeid and N. Bisnik, "Geographic protocol information and capacity deficit in mobile wireless ad hoc networks," *Information Theory, IEEE Transactions on*, vol. 57, no. 8, pp. 5133–5150, Aug 2011.

[12] "Request for information, novel methods for information sharing in large scale mobile ad-hoc networks, defense advanced research projects agency (darpa)," .

[13] Birsen Sirkeci-Mergen and Anna Scaglione, "Randomized space-time coding for distributed cooperative communication," *Signal Processing, IEEE Transactions on*, vol. 55, no. 10, pp. 5003–5017, 2007.

[14] Yun Li, Zhenghua Zhang, Chonggang Wang, Weiliang Zhao, and Hsiao-Hwa Chen, "Blind cooperative communications for multihop ad hoc wireless networks," *Vehicular Technology, IEEE Transactions on*, vol. 62, no. 7, pp. 3110–3122, Sept 2013.

[15] J. Sanchez, P. Ruiz, and R. Marin-Perez, "Beacon-less geographic routing made practical: Challenges, design guidelines, and protocols," *IEEE Commmunications Magazine*, vol. 47, Issue 8, pp. 85–91, August 2009.

[16] H. Füssler, J. Widmer, M. Käsemann, M. Mauve, and H.Hartenstein, "Contention-based forwarding for mobile ad-hoc networks," *Elseviers Ad Hoc Networks*, vol. 1, Issue 4, pp. 351–369, November 2003.

[17] M. Rossi, N. Bui, and M. Zorzi, "Cost- and collision-minimizing forwarding schemes for wireless sensor networks: Design, analysis and experimental validation," *IEEE Trans. on Mobile Computing*, vol. 8, no. 3, pp. 322–337, March 2009.

[18] N. Bisnik and A.A. Abouzeid, "Queuing delay and achievable throughput in random access wireless ad hoc networks," in *Sensor and Ad Hoc Communications and Networks, 2006. SECON '06. 2006 3rd Annual IEEE Communications Society on*, Sept 2006, vol. 3, pp. 874–880.

[19] Nabhendra Bisnik and Alhussein A. Abouzeid, "Queuing network models for delay analysis of multihop wireless ad hoc networks.," *Ad Hoc Networks, Elsevier*, vol. 7, no. 1, pp. 79–97, Jan 2009.

[20] T. Rappaport, *Wireless Communications: Priciples and Practice*, Prentice Hall, 2nd edition, 2001.

[21] M. Slavik and I. Mahgoub, "Spatial distribution and channel quality adaptive protocol for multihop wireless broadcast routing in vanet," *Mobile Computing, IEEE Transactions on*, vol. 12, no. 4, pp. 722–734, April 2013.

[22] C. Athaudage, "BER sensitivity of OFDM systems to time synchronization error," *The 8th International Conference on Communication Systems (ICCS'02), Singapore*, vol. 1, pp. 42–46, November 2002.

[23] Jianjun Ran, R. Grunheid, H. Rohling, E. Bolinth, and R. Kern, "Decision-directed channel estimation method for ofdm systems with high velocities," in *Vehicular Technology Conference, 2003. VTC 2003-Spring. The 57th IEEE Semiannual*, April 2003, vol. 4, pp. 2358–2361 vol.4.